Silicon (2022) 14:12599–12605
https://doi.org/10.1007/s12633-022-01959-2

ORIGINAL PAPER

Influence of Laser Annealing of Silicon Enriched SiOx Films on their Electrical Conductivity

O. Pylypova[1] · S. Antonin[2] · L. Fedorenko[2] · Ya Muryi[1] · V. Skryshevsky[1] · A. Evtukh[1,2]

Received: 11 February 2022 / Accepted: 10 June 2022 / Published online: 18 June 2022

Abstract

The influence of laser annealing on structural transformation and electrical conductivity of amorphous non-stoichiometric SiO_x thin films have been studied. It was found that the average sizes of silicon nanocrystals (NCs) increases from 6 nm in initial films up to 35 nm in modified one after structure transformation of SiO_x film into nanocomposite SiO_2(Si) one containing Si nanoclusters in oxide matrix after annealing by nanosecond pulses of the Nd^{+3}: YAG laser irradiation with wavelengths of 1.064 μm and 0.532 μm. It has been shown that the size of the NCs and their size distribution depend on the intensity and wavelength of laser radiation.

The significant influence of laser annealing on electrical conductivity has been revealed and explained based on structural transformation of the film. It was shown that electron transport mechanism through SiO_x films before and after laser annealing depend as on electric field and measurement temperature.

Keywords Electrical conductivity · Laser annealing · Nanocomposite film · Nanoparticles · Silicon oxide

1 Introduction

In recent years, interest in studying of the processes of crystalline nanoparticles formation and their properties has increased significantly. Moreover, it was studied not only directly themselves nanocrystals (NCs) [1–4], but the processes leading to the amorphous-crystalline phase transitions. In particular, this refers to the transformation of thin layers of SiO_x [5] and TiO_x [6] oxides into nanocomposite layers. The latter are of interest both in terms of increasing the absorption coefficient and the possible transformation of absorption spectra in order to increase the efficiency of solar energy converters, improve the characteristics of nanocatalysts and increase the sensitivity of sensors.

Isothermal annealing of films is traditionally used to study the possibilities of improving the structure and modifying their properties. However, in many cases, the more effective method of modifying the properties of films can be adiabatic laser annealing [7, 8]. The main advantages of the latter are that it is not an inertial heat source, it has a large dynamic range of intensity of the irradiation and the ability to localize its action in space (active zone) and time (duration of influence). However, there are not many works that would have studied the influence of laser annealing on electrical properties of SiO_x films that is very important for various applications.

Therefore, the main aim of our work was to study in detail the changing of electrical conductivity of laser-annealed SiO_x films as a result of their structural transformation when varying the intensity and wavelength of laser pulses.

2 Experimental

Silicon enriched SiO_x films were deposited on n-type Si substrate ($\rho = 0.01\ \Omega \times cm$) by Low Pressure Chemical Vapor Deposition (LP CVD) method at the temperature of 660 °C. The thickness of the films determined with ellipsometry at $\lambda = 632.8$ nm was 130 nm. The study of changes in surface morphology of SiO_x layers was carried out by comparing their characteristics before and after laser irradiation. The study of morphology of the films was carried out using an

✉ O. Pylypova
steblolia@gmail.com

[1] Institute of High Technologies, Taras Shevchenko National University of Kyiv, 60 Volodymyrska Str, Kyiv 01033, Ukraine

[2] V.E. Lashkaryov Institute of Semiconductor Physics NAS of Ukraine, 41 Pr. Nauki, Kyiv 03028, Ukraine

atomic force microscope (ACM) (Nanoscope IIIa, Digital Instruments, Santa Barbara).

Initial SiO_x layers were irradiated with nanosecond pulses of Nd^{+3}:YAG laser with Q-quality, the wavelengths of the irradiation were 1.064 μm and 0.532 μm. The duration of the individual pulse (t_p) was 10 ns. To determine the threshold laser intensities that lead to the structural changes in SiO_x layers, their irradiation was performed by single pulses in the X-Y scan mode with varying speed of pulse repetition and the degree of laser beam overlap. The pulse energy was $E \leq 100$ mJ. The intensity of the laser pulse was regulated by the wedge-shaped packet, assembled from the glass plates and focusing systems, and varied in the range from 1 to 114 MW / cm^2.

The measurements of current-voltage (I-U) characteristics of the initial film (after deposition) and after laser annealing have been performed by an automated complex consisting of a universal device Keithley Source Meter Series 2410. The electrical conductivity was investigated for three key intensities of laser irradiation, namely 10 MW / cm^2, 50 MW / cm^2 and 100 MW / cm^2. The measurement of electrical conductivity was performed in wide temperature range (95 K - 350 K).

3 Results and Discussion

3.1 Structural Transformation

The AFM images of the film surfaces are shown in Fig. 1 before (a) and after (b, c) laser irradiation. The dimensions of surface heterogeneities on the initial SiO_x film surface do not exceed 6 nm. After the laser irradiation of SiO_x films, the dimensions of the heterogeneities on its surface are significantly increased (Fig. 1, b).

However, the thresholds for the intensity of radiation, at which structural changes in the film began, differ significantly for both wavelengths. For the case of the action on the film by pulses with $\lambda_1 = 1.064$ μm, morphological changes on its surface began at $I = 14$ MW / cm^2, and under the action

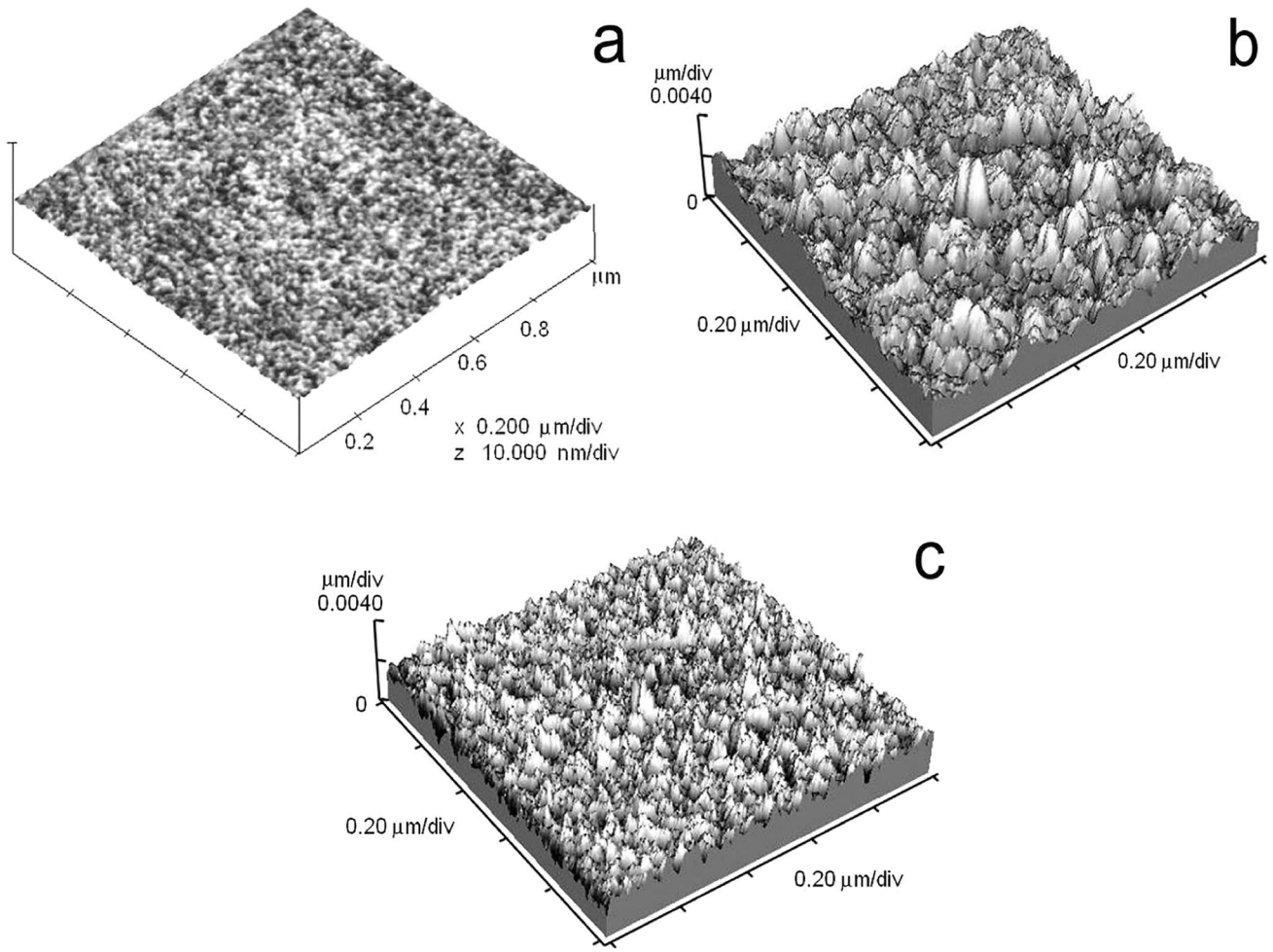

Fig. 1 AFM images of SiO_x film before (**a**) and after (**b**, **c**) - laser irradiation: b) topography, c) phase ($\lambda = 0.532$ μm, $t_p = 10$ ns, $I = 31$ MW/cm^2)

of pulses with $\lambda_2 = 0.532$ μm, already at $I = 7$ MW / cm^2. In addition, for different wavelengths, the thresholds for visually detected damages of the films is also significantly different. This is due to the large difference between the absorption coefficients ($\alpha_1 = 10$ cm^{-1}, $\alpha_2 = 10^4$ cm^{-1}) for two laser wavelengths ($\lambda_1 = 1.064$ μm, $\lambda_2 = 0.532$ μm), respectively, at not very high levels of radiation intensity. The nanostructure sizes were increasing from 6 nm to 65 nm at the variation of laser pulses intensity from 1 to 114 MW / cm^2 for $\lambda_1 = 1.064$ μm, and from 6 nm to 35 nm for $\lambda_2 = 0.532$ μm.

As it was shown earlier [8], laser annealing of an initial non-stoichiometric SiO_x film containing amorphous silicon clusters and small Si nanocrystals ($d < 6$ nm) is transformed into a nanocomposite film consisting of Si NCs having substantially larger sizes ($d > 10$ nm) and they are in the SiO_x matrix, and the value of x is close to the value in the stoichiometric SiO_2. The results of the AFM studies indicate an increase in the size of the NCs from $d \sim 6$ nm in the initial films up to $d \approx 35$ nm in the films that were acted with impulses with $\lambda_2 = 0.532$ μm and an intensity ≥100 MW/cm^2.

3.2 Electrical Conductivity

The laser annealing allows to locally affect the structure of the initial SiO_x film, causing phase transformations in it and thus influences on the conductivity of the films. It should be noted the features of the SiO_2(Si) composite obtained after laser annealing. The Fermi level of the structural phases, which stay in contact, is located at the same level. This leads to a corresponding redistribution of charges between them. The conductivity and electron transport mechanisms were determined for the SiO_x films annealed by laser with $\lambda_2 = 0.532$ μm and intensities of $I = 10$ MW/cm^2, $I = 50$ MW/cm^2, and $I = 100$ MW/cm^2, respectively.

Laser irradiation with intensity of 10 MW/cm^2. The dependences of electrical conductivity on voltage are presented in (Fig. 2a). As can be seen, four different regions can be distinguished in dependence on the voltage and temperature: I – low voltage region ($U < 0.2$ V, $250 < T < 350$ K), II – medium voltage region ($0.2 < U < 1$ V, $180 < T < 350$ K), III – medium voltage region ($0.2 < U < 1$ V, $101 < T < 107$ K), IV – high voltage region ($U > 2$ V).

In the *region I*, the hopping with variable length conductivity mechanism dominates [9], as evidenced by the approximation of dependences in Mott coordinates (Fig. 3). The hopping occurs at adjacent energy levels, which are near the Fermi level. To determine the density of localized electron states $N(E_F)$, the average hopping length R_{hop} and the hopping activation energy $W_{hop}(T)$ of localized states near the Fermi level, we used the analysis described in [10]. In the case of laser irradiation with $I = 10$ MW / cm^2, the density of states is equal to $N(E_F) = 4.21 \times 10^{17}$ cm^{-3} at $E = 2.3 \times 10^4$ V / cm, and the $R_{hop} = 1.3 \times 10^{-6}$ cm at $T_1 = 288$ K and.

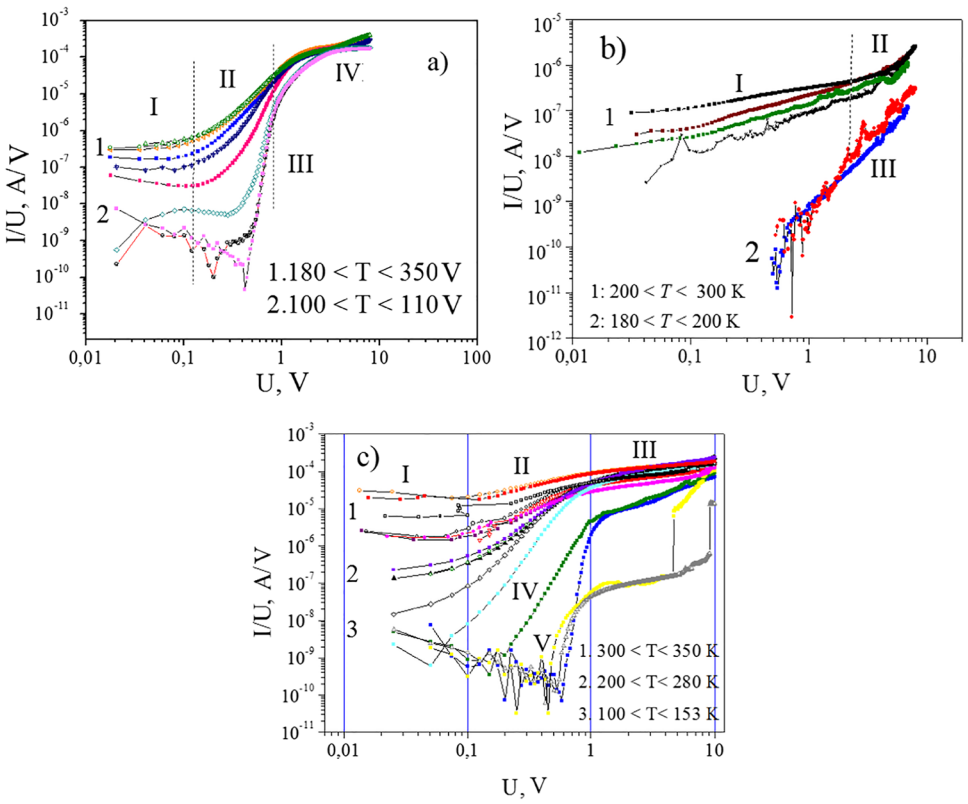

Fig. 2 I/U – U characteristics of SiO_x films after laser annealing with intensity of **a**) 10 MW / cm^2, **b**) 50 MW / cm^2, **c**) 100 MW / cm^2. Measurement temperature as a parameter

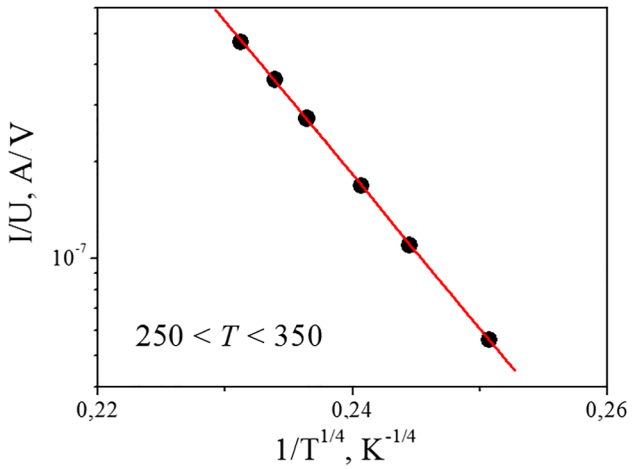

Fig. 3 Conductivity in Mott coordinates after laser irradiation ($I = 10$ MW / cm^2)

$R_{hop} = 1.24 \times 10^{-6}$ cm at $T_2 = 330$ K. As the measurement temperature increases, the hopping length decreases. The hopping activation energy increases with the temperature growth: $W_{hop} = 0.165$ eV at $T_1 = 288$ K and $W_{hop} = 0.18$ eV at $T_2 = 330$ K, respectively.

For *region II* ($0.2 < U < 1$ V, $180 < T < 350$ K) the conductivity corresponds to space charge limited current (SCLC) mechanism with electron injection and shallow traps [10–13] for all measurement temperatures (Fig. 4). According to this mechanism based on analysis presented in [10], the characteristic temperature T_t, the characteristic energy E_t of the trap distribution and the concentration of trapping state N_t were calculated. Initially, the concentration of traps was determined. As can be seen from Fig. 4a, the "crossing voltage" U_c of characteristic curves in log I - log U coordinates is equal to 0.86 V. The dependence of power in the relation describing SCLC [10] on reciprocal temperature shown in Fig. 4b. It should be noted that with the temperature growth, the power m approaches to three, $I \sim U^3$. It can be assumed that $I \sim U^3$ dependence is characteristic for SiO_x film [10, 13].

The value of "crossing voltage" is defined by the expression:

$$U_c = qN_t d^2 / 2\,\varepsilon_r\,\varepsilon 0 \tag{1}$$

where ε_0 is the permittivity of free space, $\varepsilon_r = 8.1$ is the dielectric constant that was determined from capacitance-voltage (C–V) characteristics, d is the film thickness.

The density of traps $N_t = 7.23 \times 10^{16}$ cm^{-3} was determined according to eq. $_1$. The values of characteristic temperature $T_t = 435$ K, characteristic energy $E_t = 0.037$ eV were determined from curve slope in Fig. 4a.

The analysis of the SiO_x film conductivity after laser annealing in the *region III* indicates the conductivity according to the Poole-Frenkel (P-F) mechanism [14] describing by the expression:

$$I \sim U \exp\left[-\frac{q\varphi_B}{kT} + \frac{q\sqrt{qU/d\pi\varepsilon_r\varepsilon_0}}{kT}\right] \tag{2}$$

where $q\varphi_B$ is the depth of the electron traps.

The dependences of the conductivity in the P-F coordinates are presented in Fig. 5a. From the slope of this curve, the depth of traps in the SiO_x film in relation to bottom of conduction band $q\varphi_b \approx 0.17$ eV was determined.

Laser Irradiation with Intensity of 50 MW/cm^2 There are three distinguished regions in *t*he dependences of electrical conductivity on voltage after laser annealing with an intensity of 50 MW/cm^2: I – low voltage region ($U < 0.2$ V, $200 < T < 300$ K), II - high voltage region ($U > 2$ V, $200 < T < 300$ K), III – high voltage region ($U > 2$ V, $180 < T < 200$ K) (Fig. 2b).

In *region I* the quadratic dependence of current on voltage $I \sim U^2$ is observed. $I \sim U^2$ dependence corresponding to pace charge limited current (SCLC) mechanism This means that in a temperature range of $200 < T < 300$ K (Fig. 2b, region

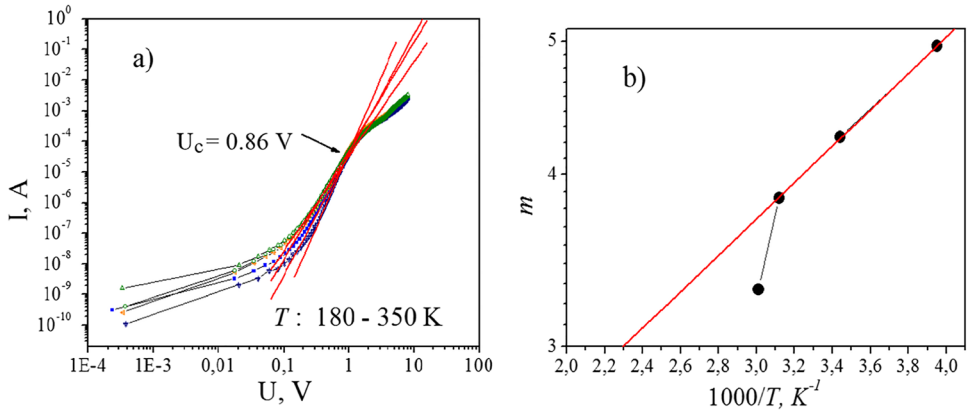

Fig. 4 (**a**) The fitting of the I-U characteristic in the temperature range 180–350 K. (**b**) The power m as a function of reciprocal temperature for the same temperature range

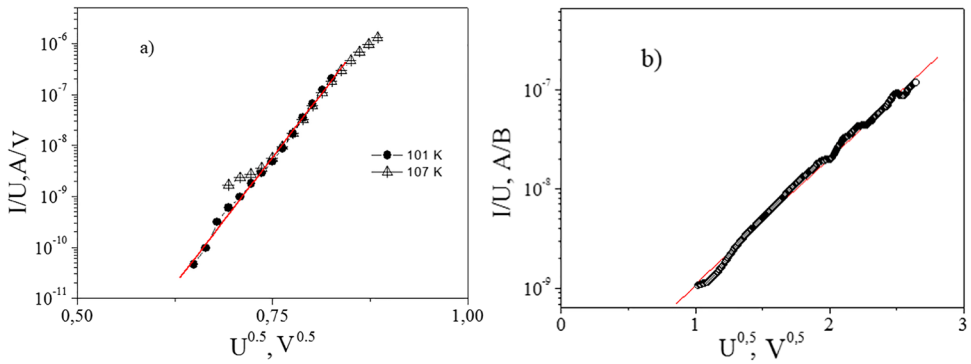

Fig. 5 I – U characteristics in Poole-Frenkel coordinates for SiO_x films after laser annealing: a) $I = 10$ MW/cm^2, b) $I = 50$ MW / cm^2

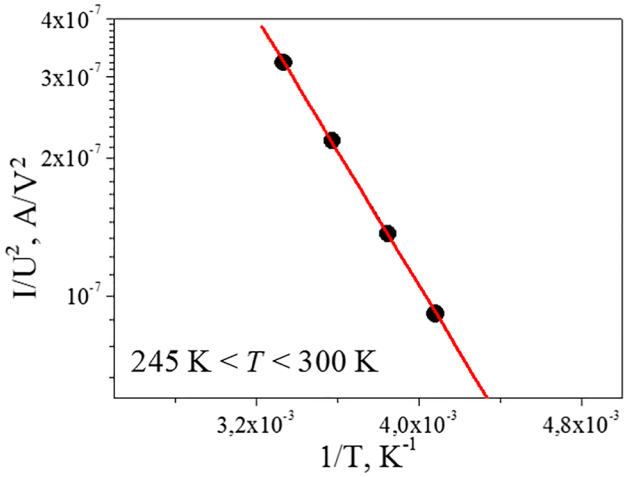

Fig. 6 I – U characteristics in Arhenius coordinates ($I = 50$ MW / cm^2)

I) monoenergetic traps located above the Fermi level [10, 13]. The energy level of the traps involved in the transport of carriers $E_{tм} - E_F = 0.14$ eV was calculated from the slope of the curve shown in Fig. 6 in the Arrhenius coordinates. In this case, they are located at ~0.14 eV above the Fermi level.

The I – U characteristics in the *region II* ($U > 2$ V, $200 < T < 3\,00$ K) show the power dependence $I \sim V^m$, where $m > 2$. The "crossing voltage" in this case is $V_c = 9.7$ V. Using expression (1) we calculate the concentration of electron traps $N_t = 2.46 \times 10^{17}$ cm^{-3}. The characteristic temperature $T_t = 303$ K and the energy of the traps $E_t = 0.026$ eV were determined from curve slope.

In the *region III* ($U > 2$ V, $180 < T < 200$ K) there is the P-F mechanism of conductivity (Fig. 5b).

The level of traps $q\varphi_b = 0.37$ eV (calculated from the bottom of the conduction band) were determined from the slope of the curve. The determined value of the level of traps shows that with increasing intensity up to 50 MW / cm^2, the barrier increases, and accordingly the influence of states near the Fermi level on current transport decreases, which is associated with the decrease of their density and the increase in silicon nanoinclusions as a result of structure transformation.

Laser Irradiation with Intensity of 100 MW/cm^2 The laser irradiation of the film with the intensity of 100 MW / cm^2 transforms SiO_x film into nanocomposite SiO_2(Si) one containing silicon nanoinclusions into oxide matrix.

For the low voltage *region I* ($U < 0.1$ V) the I – U characteristics can be divided into two intervals depending on the measurement temperature of $180 < T < 300$ K and $300 < T < 350$ K (Fig. 2c). For the average temperature range of $180 < T < 300$ K, the quadratic dependence of the current on the voltage is observed. The conductivity in the structure is determined by one group of monoenergetic traps located above the Fermi level [10, 13]. A similar dependence is observed in the *region V* of the I – U characteristics. The calculated values of energy level of the traps involved in the carriers transport E_t were obtained from the slope of the curves in the Arrhenius coordinates and are given in Table 1. At lowering measurement temperatures from 350 to 200 K, the Fermi level rises by 0.09 eV to the bottom of the conduction band.

For high temperatures of $300 < T < 350$ K, the conductivity according to Mott's law is realized.

For the *region II* in temparature range $300 < T < 350$ K there is the quadratic dependence of current on voltage corresponding to SCLC mechanism.

For the *region III* ($U > 2$ V, $200 < T < 350$ K) the dependence of current on voltage is $I \sim U^{3/2}$. Such dependence corresponds the case when the drift velocity of the carriers depends only on the field, which is characteristic of the so-called "warm" electrons. In this case scattering by acoustic phonons predominates [[12];].

In the *region IV* ($U < 1$ V, $100 < T < 160$ K) the electron tunneling mechanism predominates. From the slope of the curves in the Fowler-Nordheim coordinates, we determined the value of the barrier, which is equal to $q\varphi = 0.1$ eV. The field at low voltages has little effect on the barrier height, which means that direct tunneling through oxide layers between nanocrystals predominates.

Table 1 The parameters of the conduction mechanisms of SiO_x and SiO_2(Si) films after laser annealing

I, MW/cm^2	*T*, K	*U*, V	Mechanism	Parameters
10	250–350	< 0.2	Mott	$N(E_F)=4.21\times10^{17}$ eV^{-1} cm^{-3}; $R_{hop}=1.3\times10^{-6}$ cm (288 K); $W_{hop}=0.165$ eV (288 K)-
	180–350	$0.2<U<2$	SCLC	$W_{hop}=0.059$ eV; $V_c=0.86$ V; $N_t=7.25\times10^{16}$ cm^{-3}; $T_t=435$ K; E_t, = 0,037 eV
	100–110	$0.2<U<2$	P-F	$q\varphi_b=0.17$ eV
	100–350		$U^{1/5}$	
50	245–300	< 2	U^2	$E_c=0.14$ eV
	245–300	> 2	SCLC	$V_c=9.3$ V; $N_t=2.44\times10^{17}$ см$^{-3}$; $T_t=303$ K; E_t, = 0.026 eV
	180–200	>4	P-F	$q\varphi_b=0.37$ eV
I, MW/cm^2	*T*, K	*U*, V	Mechanism	Parameters
100	300–350	< 1	Mott	$N(E_F)=9.31\times10^{13}$ eV^{-1} cm^{-3}; $R_{hop}=2.1\times10^{-4}$ cm (300K); $W_{hop}=1.5$ eV
	200–350	$0.2<U<1, >2$	SCLC, $U^{1/5}$	$V_c=0.58$ V; $N_t=1.51\times10^{16}$ см$^{-3}$; $T_t=357$ K; E_t, = 0.03 eV
	200–300	<0,1	U^2	$E_c=0.12$ eV
	100–160	< 1	F-N	$q\varphi_b=0.1$ eV

All obtained parameters characterizing the conductivity through SiO_x films depending on the power of the laser radiation, voltage range and measurement temperatures are summarized in Table 1.

4 Conclusions

The effect of laser annealing on the peculiarities of electric conductivity of silicon-enriched SiO_x films as a result of their transformation into a nanocomposite SiO_2(Si) film containing Si NC in the dielectric matrix has been investigated in detail. The possibility of laser-induced nanostructural transformation of non-stoichiometric thin SiO_x-amorphous films containing Si NCs with initial averaging values of $d \leq 6$ nm into the SiO_2 nanocomposite layer with increased NCs sizes, $d \sim 35$ nm was shown based on the analysis of AFM images. The physical model that explains the increase in the size of Si NCs in thin SiO_x films has been considered. It was shown that electron transport mechanism through SiO_x film depend as on electric field and measurement temperature. The main electron transport mechanisms are hopping with variable length (Mott't mechanism), electric field enhance thermal excitation of electron from the traps into conduction band (Poole-Frenkel mechanism), space charge limited current (SCLC) and electron tunneling. The significant influence of laser annealing on electrical conductivity has been revealed and explained based on structural transformation of the film. Structures with silicon nanoparticles that are grown inside SiO_2 matrix draw researchers' attention due to prospects of creation on their basis functionally new nanoelectronics devices such as nanocrystal memory, single-electron transistors, Si-based LEDs and laser. As a rule, the SiO_2(Si) films containing Si nanoclusters are formed during high temperature annealing in the furnace. The using of the laser annealing allows to form Si nanocluster locally on small part of the wafer. This feature is very attractive for nanotechnology and creation of nanodevices.

Author Contributions The manuscript was written through the contributions of all co-authors. All authors have approved the final version of the manuscript.

Data Availability Data will be available on request.

Declarations

Consent for Publication All authors of the article agree to participate in the publication.

Consent to Participate All authors of the article agree to participate in the publication.

Ethics Approval The authors declare that the work is written with due consideration of ethical standards.

Research Data Policy The authors declare that data supporting the findings of this study are available within the article.

Conflict of Interest The authors declare that they have no conflicts of interest.

Research Involving Human Participants and/or Animals Not applicable.

References

1. Kizjak AY, Evtukh AA, Bratus OL et al (2022) Electron transport through composite SiO2(Si)&FexOy(Fe) thin films containing Si and Fe nanoclusters. J Alloys Compd 903:163892. https://doi.org/10.1016/j.jallcom.2022.163892
2. Koike R, Suzuki R, Katayama K, Higashihata M, Ikenoue H, Nakamura D (2021) Observation of SiO_2 nanoparticle formation

via UV pulsed laser ablation in a background gas. JLMN. https://doi.org/10.2961/jlmn.2021.03.2006
3. Mandal S, Gupta AK, Echeverria E et al (2022) Laser-assisted nanofabrication of multielement complex oxide Core-Shell nanoparticles. SSRN Journal. https://doi.org/10.2139/ssrn.4084712
4. Ruffino F, Grimaldi MG (2019) Nanostructuration of thin metal films by pulsed laser irradiations: a review. Nanomaterials 9:1133. https://doi.org/10.3390/nano9081133
5. Taheri M, Mansour N (2020) Silicon nanoparticles produced by two-step nanosecond pulsed laser ablation in ethanol for enhanced blue emission properties. Silicon 12:789–797. https://doi.org/10.1007/s12633-019-00168-8
6. Al-Kamal AK (2015) Synthesis of Ag-doped TiO_2 NPs by Combining Laser Decomposition of Titanium Isopropoxide and Ablation of Ag For Dye-Sensitized Solar Cells. Master of Science thesis. The State University of New Jersey
7. Fedorenko LL, Prudnikov AM, Evtukh AA et al (2018) Laser-stimulated phase transformations in thin layers of SiOx and CNx –Ni. Mater Sci 54:223–229. https://doi.org/10.1007/s11003-018-0177-0
8. Steblova OV, Fedorenko LL, Evtukh AA (2017) Nanostructuring the SiOx layers by using laser-induced self-organization. Semicond Phys Quantum Electron Optoelectron 20(179–184):10.15407/spqeo20.02.179
9. Mott NF, Davis EA (1979) Electronic processes in non-cristalline materials. Oxford University Press, Oxford
10. Kizjak A, Evtukh A, Steblova O, Pedchenko Y (2016) Electron transport through thin SiO2 films containing Si nanoclusters. J Nano Res 39:169–177. https://doi.org/10.4028/www.scientific.net/JNanoR.39.169
11. Grillo A, Giubileo F, Iemmo L et al (2019) Space charge limited current and photoconductive effect in few-layer MoS_2. J Phys Conf Ser 1226:012013. https://doi.org/10.1088/1742-6596/1226/1/012013
12. Kao KC, Hwang W (1984) Electrical transport in solids. Pergamon Press, New York
13. Lampert MA, Schilling RB (1970) Current injection in solids: the regional approximation method. Semicond Semimetals 6:1–96. https://doi.org/10.1016/S0080-8784(08)62630-7
14. Sze SM (1981) Physics of semiconductor devices. John Wiley & Sons Inc., New York